Designs of the Monopole Slot Antenna Arrays Operated at the WLAN Band

Chun-Ming Lin, Yang Tai, Kai-Long Hsiao, and Chien-Jen Wang
Department of Electrical Engineering, National University of Tainan, Tainan, Taiwan
E-mail: cjwang@mail.nutn.edu.tw

***Abstract*—Design procedures of two-element monopole slot antenna arrays are presented in this paper. We proposed several array topologies utilizing different feeding structures and injecting in-phase or out-of-phase signals to achieve power-combining radiation patterns. The sum and difference radiation patterns are successfully achieved and are theoretically analyzed. Furthermore, the power-combining characteristics are also presented by two proposed antenna arrays. The proposed antenna arrays can be candidates of the radiator for the base station or access point of the wireless local area network system.**

***Index Terms*—monopole slot antenna, beam-scanning, power-combining.**

I. INTRODUCTION

Generally speaking, by arranging several antennas in space and interconnecting to produce a directional radiation pattern, such a configuration of multiple radiating elements is referred to as an antenna array. An array offers the important advantages of a high antenna gain, a narrow beam width, low side lobe, and an electronically scanning beam [1]. In [2], the analysis is shown that for identical elements separated by an integral number of half wavelengths, stability can be predicted, with no additional information required, such that the good mutual coupling effect can be derived. Many past researches have been proposed for discussions and improvement of the power combining characteristics [3-5]. For example, in [3], a lower sidelobe antenna array was demonstrated by utilizing a 16-element linear array. The factors affecting the sidelobe characteristics of the array were examined. In 1993, York proposed a new technique for phase-shifterless beam-scanning by using couple-oscillator array. By tuning the frequencies of the end oscillators in the chain, the main beam could be steered over a range of angle 37^{o}. A unilateral injection-locking active antenna array with electronic scanning performance was proposed in [5]. With a frequency tuning range of 30 MHz, the measured scanning range was 21^{o}, approximately. The cost of the scanning antenna array could be reduced.

Recently, the monopole slot (or open slot) antenna attracts much attention due to its compact size for a fixed operating frequency. A quarter-wavelength monopole slot cut in the finite ground plane and fed by a microstrip transmission line, a wide impedance bandwidth and bi-directional radiation are provided [6-10]. It is different from the conventional shorted slot antenna resonating at a half-wavelength. Hence, the monopole slot antenna can occupies some value spaces on the system circuit board. Due to the monopole topology [6], co-polarized radiation patterns of the monopole slot antenna at different frequencies look omni-directional. Several different slot shapes were introduced to generate additional resonances so that bandwidth enhancement was achieved [7]. Furthermore, the occupied area of the antenna was decreased. In [8], a pentagon-shape slot was etched as a radiator on the ground plane, and a feeding line with a pentagon stub was used. This antenna demonstrates a superior ultra-wideband (UWB) impedance bandwidth. In [9], a simple folded slot was etched as a radiator on the ground plane, and a feeding line with a connecting strip was used. This antenna covers penta bands of WWAN operation and is suitable to be placed at the hinge of the clamshell mobile phone. Due to the radiation from a notch embedded in the ground plane, for the monopole slot antenna, the beams in the broadside cut planes are quasi-omnidirectional and the beamwidth are wide. A switched-beam antenna array has been demonstrated in [10]. The proposed antenna is mainly composed of a four-element array with radiation elements based on the L-shaped monopole slot antenna. By controlling four pin diodes of a single-pole-four-throw (SP4T) switch, switched-beam radiation patterns for WLAN applications are obtained in one plane. However, the main beam of the beam-switched antenna array can not continuously scan in the free space. Moreover, the beam shape is fan-like and the beamwidth seems too wide for target searching function.

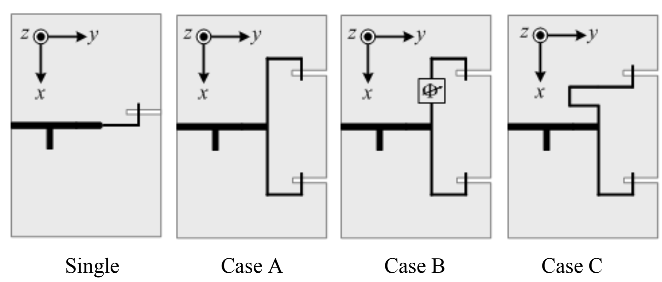

Fig. 1 Configuration of four monopole slot antenna case. (Single, Case A, B, and C)

In this paper, beam-scanning antenna arrays based on two identical monopole slot antennas are shown. Two straight slots are cut at the edge of the finite ground plane of a microstrip structure. The radiating element is a rectangular slot of total length 0.25 λ_g to achieve a compact design. From the results of radiation characteristics, power combining characteristics and mutual coupling effect between the two monopole slots are studied and analyzed by two proposed antenna arrays. Furthermore, three linear arrays of two identical antenna elements with two distinct modes: in-phase or anti-phase (out-of-phase), are shown, and thus an identification of which mode the array will be operating in, depending on the phase difference of the input signals, can be ascertained prior to an array construction.

II. Configurations of Antenna Structure

Configuration of four monopole slot antenna case. (Single, Case A, B, and C) are shown in Fig. 1. The conventional single slot antenna and dimensional parameters are shown in Fig. 2. The tested antennas in our experiment are printed on a circuit board material such as FR-4 substrate ($\varepsilon_r = 4.4$, tan $\delta = 0.02$, h = 1.6 mm), and fed by a high-impedance feeding line of width 0.7 mm. A monopole slot is cut at the edge of the finite ground plane of a microstrip structure. Its length, S_L = 20 mm is approximately a quarter guided wavelength at 2.4 GHz. The ground plane for each following case has a size of 150 × 100 mm^2. In order to decrease the impedance mismatching condition due the high impedance of the slot antenna, an open-circuited tuning stub is connected to a 50-Ω microstrip transmission line.

Fig. 3 illustrates a linear array (Case A) of two identical radiating elements with an anti-phase signal injection. Each element is designed to have the same dimensions as the single slot antenna in Fig. 2. A T-junction power divider is used to provide equal power for wideband operation, where each half of the input signal is injected into the input port of the monopole slot antennas. The feeding ports at the two slot edges are in opposite directions. Two antenna elements are separated by one half of the free-space wavelength in order to yield any desired directivity [11]. It is noted that the phase of the signal at the input port of each slot is equal (in-phase). The second array topology (Case B) is shown in Fig. 4. The difference between the two arrays is adding a phase shifter which controls the phase difference of the input signals at the two input ports. In order to change the phase difference between the radiating elements, a pair of phase shifters was designed and fabricated to modulate the phase of each input signal.

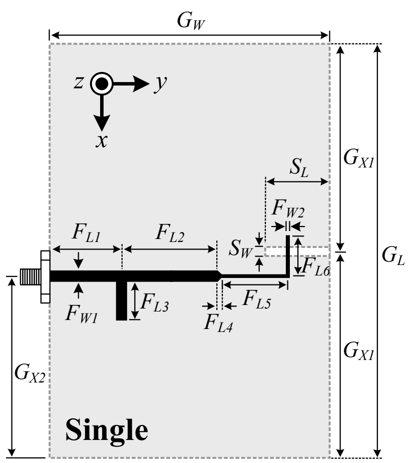

Parameter	(mm)
G_L	150
G_W	100
S_L	20
S_W	3
G_{X1}	75
G_{X2}	66.6
F_{L1}	41.7
F_{L2}	22.15
F_{L3}	12.5
F_{L4}	1.15
F_{L5}	20.35
F_{L6}	12.65
F_{W1}	3
F_{W2}	0.7

Fig. 2 Configuration of a conventional single monopole slot antenna.

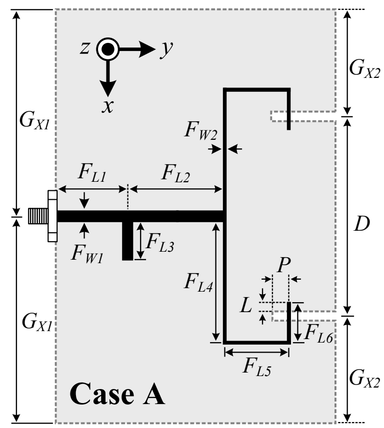

Parameter	(mm)
G_{X1}	75
G_{X2}	43.75
D	62.5
F_{L1}	43
F_{L2}	22
F_{L3}	11.2
F_{L4}	38.15
F_{L5}	20
F_{L6}	12.65
F_{W1}	3
F_{W2}	0.7
L	2.75
P	5

Fig. 3 Linear array of Case A.

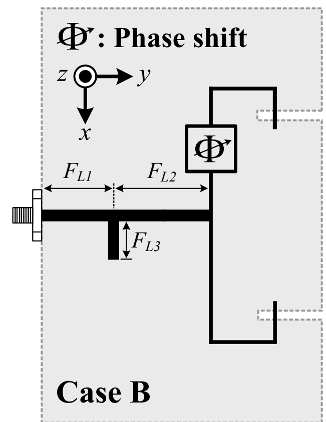

Parameter	(mm)
F_{L1}	41.7
F_{L2}	23.3
F_{L3}	7.6

Fig. 4 Linear array of Case B.

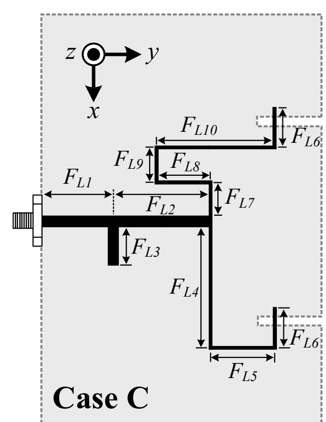

Parameter	(mm)
F_{L1}	40.6
F_{L2}	24.4
F_{L3}	7.2
F_{L4}	38.15
F_{L5}	20
F_{L6}	12.65
F_{L7}	12.65
F_{L8}	8.05
F_{L9}	8.7
F_{L10}	28.05

Fig. 5 Linear array of Case C.

Here, the phase difference is set by 180 degree. The arrangement of the feeding network is unchanged. Fig. 5 presents the third array topology (Case C). The feeding ports are changed and arranged in the same direction. The electric lengths of the transmission lines between the feeding port of upper slot element and the node of the divider are equal. Hence, the phase difference between the signals of the two feeding ports is zero.

III. Result and Discussions

To carry out the Finite Element Method (FEM) investigation, this study uses the High Frequency Structure Simulator (HFSS) commercial software from Ansoft Corporation. Fig. 6 exhibits the comparisons of the simulated and measured reflection coefficients (S_{11}) of the four antenna structures, including the conventional single monopole slot antenna (Single) and three two-element array topologies (Case A, B, C). As can be observed from the two figures, the resonant frequencies of the four antenna structures are operated around 2.4 GHz, as predicted. The simulated and measured results agree well. The slight discrepancy between the simulated and measured results may be attributed to the fabrication misalignment and the physical value of the dielectric constant. In accordance with the measured results, the frequency band of the conventional slot antenna ranges from 2.38 to 2.46 GHz. The three antenna arrays of Cases A, B, and C achieve the bandwidths from 2.39 GHz to 2.45 GHz, from 2.36 GHz to 2.55 GHz, and from 2.34 GHz to 2.54 GHz (for S_{11} < -10 dB). The bandwidths of the latter two antenna arrays (Cases B and C) are wide than that of the single slot and the array of Case A. Furthermore, the initial resonated frequencies of the latter two arrays also shift down. phase shift is 0 degree or 180 degree.

Fig. 7 provides the comparison of the simulated radiation patterns of the single monopole slot antenna and the antenna array, Cases A. The simulated surface current densities of the four antennas structures (Single, Case A, B, and C) at 2.4 GHz are shown in Fig. 8. In Fig. 8(a), for the conventional single monopole antenna, the currents along the edges of the slot are in the opposite directions, so the currents result in the out-of-phase electric fields in free space and thus the corresponding radiations can be canceled. The useful radiation results from the currents which distribute along the right edges of the ground plane. In Fig. 7, in the xy-plane, due to the feeding network, the left space of the radiation pattern of the conventional single slot antenna is rippled. In, the xz-plane, the powers in the transverse directions of $\theta = 0^o$ and $\theta = 180^o$ are maximum because the current elements flow upward and downward.

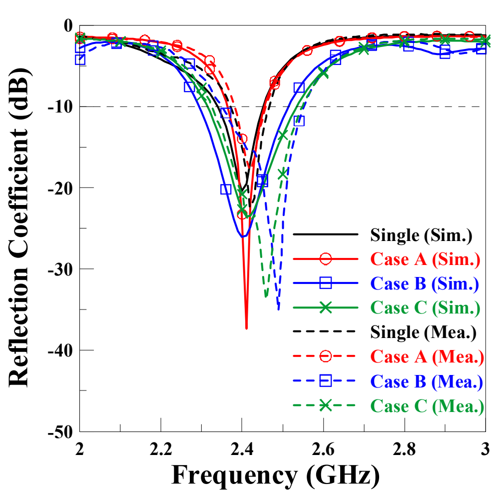

Fig. 6 Comparison of the reflection coefficients (S_{11}) of the four antenna structures. (Single, Case A, B, and C)

Hence, the radiation pattern is eight-like. From the results of Fig. 8(b), it can be seen that, for the array of Case A, two in-phase input signals cause the currents at the middle of the left side of the ground plane canceled and two out-of-phase groups of the currents can not achieve power-combining radiation. In the xy-plane radiation pattern of Fig. 7, it is observed that a difference radiation pattern with two maximum powers in the y-direction results from the two out-of-phase current groups because of the anti-symmetrical feeding structure. The out-of-phase currents also contribute to a butterfly-like radiation pattern in the xz-plane. The null points in the y- and z-directions results from the currents canceled at the middle of the ground plane. Hence, the two injected signals with equal phase are not suitable for a linear two-element monopole slot antenna array. Meanwhile, in the yz-plane, the powers of the array of Case A are much smaller than those of the single monopole slot antenna due to the cancellation of the surface currents.

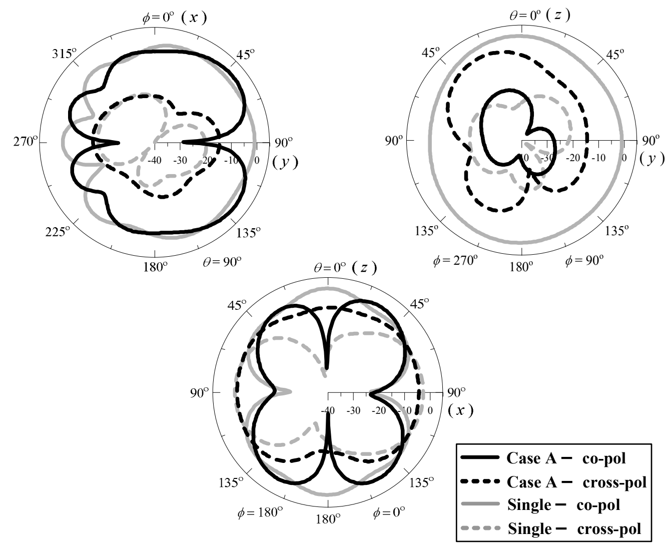

Fig. 7 Comparison of the simulated radiation patterns of the single monopole slot antenna and the array of Cases A.

Fig. 9 presents the comparison of the simulated radiation patterns of the two arrays of Case A and B. As can be observed from the figures, by utilizing an anti-symmetrical feeding structure and feeding two out-of-phase injected signals, the power-combining characteristics of the Case B array are achieved. In Fig. 8(c), the edge currents distribute in the same direction. Hence, the powers radiating from the two monopole slots successfully combine, and the main beams reconstruct. Then a sum pattern is derived, instead of a difference pattern. The radiation of the antenna array of Case B is end-fired, like a Yagi antenna. It is noted that the radiation patterns of the single slot antenna and the array of Case B are similar due to the similar current distribution. The only difference between the patterns is that the y-directional power of the array is stronger than that of the single slot antenna. It may be attributed to the current enhancement at the middle of the edge of the ground plane for the array.

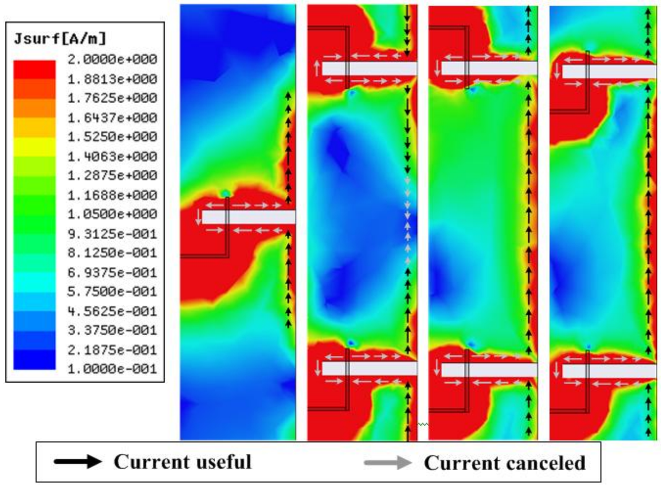

Fig. 8 Simulated surface current densities of the four antennas structures at 2.4 GHz. (a) Single (b) Case A (c) Case B (d) Case C

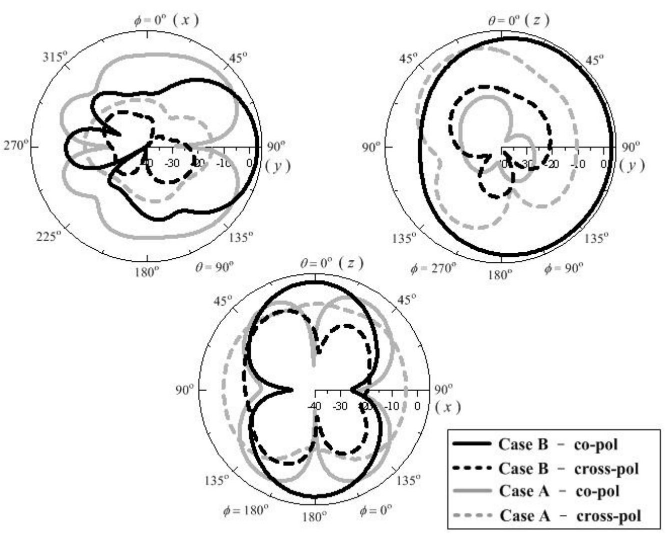

Fig. 9 Comparison of the simulated radiation patterns of the antenna arrays of Cases A and B.

Fig. 10 shows the comparison of the simulated radiation patterns of the two arrays of Case A and C. By utilizing a same-directional feeding structure and feeding two in-phase injected signals, the good power-combining characteristics of the array of Case C are achieved. It is also seen that the radiation patterns are as similar as those of the array of Case B. Table 1 lists the results of the radiation characteristics for the four antenna structures, including the conventional single slot and the three arrays (Case A, B, and C). The +y- and z-directional power intensities of the latter two arrays (Case B and C) are approximately double to that of the conventional single-slot antenna and the array of Case A due to the successful power combination in the free space. The 3dB-beamwidths of the latter two arrays in the xy- and yz-planes become sharp than those of the other two cases (Single and Case A). It is also noted that the front-to-back (F/B) power ratios of the latter two arrays are superior, compared to the first two cases.

Fig. 11 illustrates the comparison of the measured radiation patterns of the four antenna structures, including the conventional single slot and the three arrays (Case A, B, and C). As predicted, the sum patterns in the every plane successfully demonstrate good power combining capability for the arrays of Cases B and C. The maximum power-intensity point is at the end-fired (+y-direction) direction of the substrate, where is at the angle of $\theta = 90^o$ and $\phi = 90^o$. The measured beam-scanning radiation patterns of the array of Case B are shown in Fig. 12. It is noted that the phase difference of the phase shifter is varied by 90^o, 0^o, and 270^o. It is easily implemented by changing the electric lengths of the transmission lines of the T-junction power divider to achieve the phase difference. The two-dimensional electronically scanning characteristics are observed in the xy- and xz-planes. As can be seen from the figure, the radiation angle of the main beam in the xy-plane is increased from 74^o to 113^o as the phase difference is increased from 90^o to 270^o. In the xz-plane, the scanning angles of the dual beams in the +z and –z-directions are approximately 43 degrees.

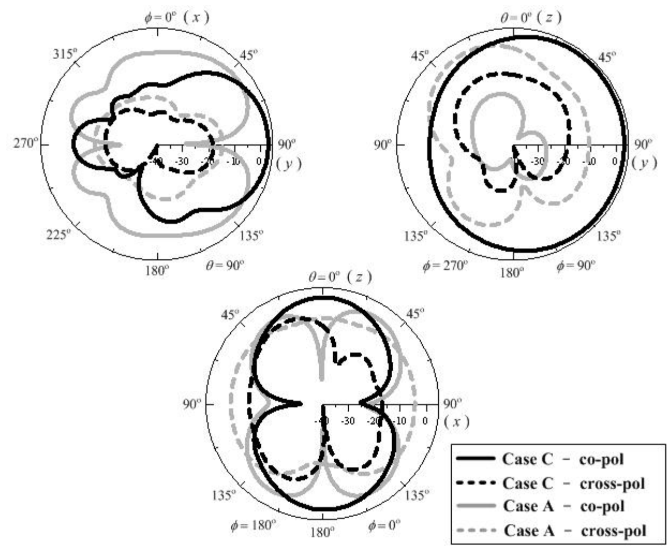

Fig. 10 Comparison of the simulated radiation patterns of the antenna arrays of Case A and C.

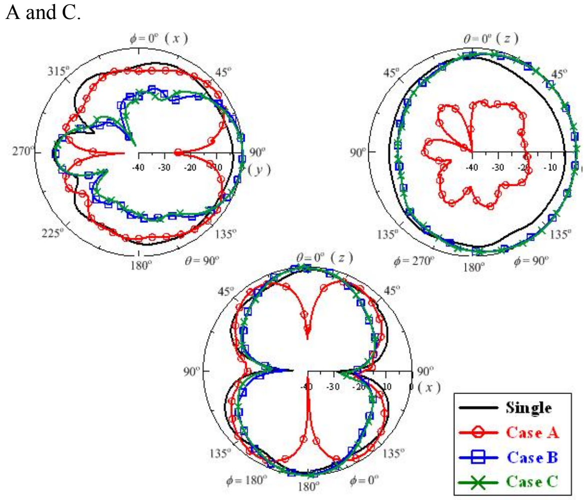

Fig. 11 Comparison of the measured radiation patterns of the four antenna structures. (Single, Case A, B, and C)

IV. CONCLUSION

This work has proposed useful techniques of power combining and mutual coupling for the monopole slot antenna array by comparing four antenna structures, including the conventional single slot and the three arrays (Case A, B, and C). One technique shown by Case B is to utilize the feeding ports in opposite directions and to inject two out-of-phase signals; on the contrast, the other technique shown by Case C is to utilize the feeding ports in the same direction and to inject two in-phase signals. The two-dimensional beam-scanning characteristics are successfully demonstrated for the array of Case B. For the antenna designers, the information of this paper will be useful to complete fabrication of the monopole slot antenna array.

Table 1. Radiation characteristics of the four antenna structures.

Parameters \ Case			Single	Case A	Case B	Case C
xy plane	Gain (dB)	+y	-0.97	-27.45	3.01	3.11
		-y	-4.09	-24.91	-8.66	-7.6
		+x	-2.74	-4.48	-19.37	-17
		-x	-3.72	-4.6	-12.92	-11.61
		F/B ratio	3.12	-2.54	11.68	10.87
	3 dB beamwidth (degree)		186	N/A	60	64
yz plane	3 dB beamwidth (degree)		286	67	211	194
xz plane	Gain (dB)	+z	0.67	-21.93	1.72	1.17
		-z	0.08	-31.66	1.57	0.89
		+x	-23.33	-21.84	-25.43	-24.64
		-x	-24.38	-19.06	-30.85	-31.44
	3 dB beamwidth (degree)		44	N/A	51	54

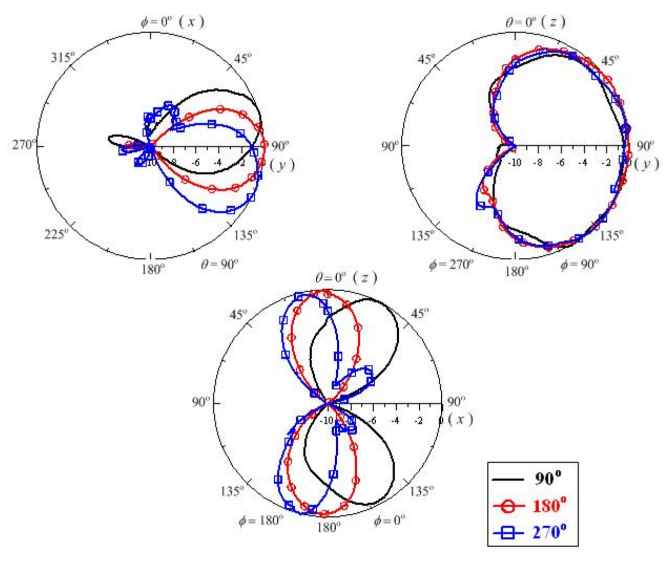

Fig. 12 Measured beam-scanning radiation patterns of the array of Case B with different phase difference (90º, 180º, 270º)

REFERENCES

[1] W. L. Stutzman and G. A. Theiele, *Antenna Theory and Design*, 2nd ed., John Wiley, 1998.

[2] D. E. J. Humphrey and V. F. Fusco, "Nonlinear two elements active antenna array stability analysis," *Electron. Lett.*, vol. 32, no. 9, pp. 788-789, Apr. 1996.

[3] D. M. Pozar and B. Kaufman, "Design considerations for low sidelobe microstrip arrays," *IEEE Trans. Antennas and Propag.,* vol. 38, no. 8, pp. 1176-1185, Aug. 1990.

[4] P. L. Liao and R. A. York, "A new phase-shifterless beam-scanning technique using arrays of coupled oscillators," *IEEE Trans. Microw. Theory Tech.*, vol. 41, no. 10, pp. 1810-1815, Oct. 1993.

[5] S. T. Chew, T. K. Tong, M. C. Wu, and T. Itoh, "An active phased array with optical input and beam-scanning capability," *IEEE Microw. Guided Wave Lett.*, vol. 4, no. 10, pp. 347-349, Oct. 1994.

[6] P. Zhao and J. Rahola, "Quarter-wavelength wideband slot antenna for 3–5 GHz mobile applications," *IEEE Antennas Wireless Propag. Lett.*, vol. 4, pp. 421–424, 2005.

[7] S. I. Latif, L. Shafai, and S. K. Sharma, "Bandwidth enhancement and size reduction of microstrip slot antenna," *IEEE Trans. Antennas and Propag.,* vol. 53, pp. 994–1003, Mar. 2005.

[8] S. K. Rajgopal and S. K. Sharma, "Investigations on ultra-wideband pentagon shape microstrip slot antenna for wireless communications," *IEEE Trans. Antennas and Propag.,* vol. 57, pp. 1353-1359, May 2009.

[9] F. H. Chiu and K. L. Wong, "Simple Folded monopole slot antenna for Penta-band clamshell mobile phone application," *IEEE Trans. Antennas and Propag.,* vol. 57, no. 11, pp. 3680-3684, Nov. 2009.

[10] M. I. Lai, T. Y. Wu, J. C. Hsieh, C. H. Wang, and S. K. Jeng, "Compact switched-beam antenna employing a four-element slot antenna array for digital home applications," *IEEE Trans. Antennas and Propag.,* vol. 56, no. 9, pp. 2929-2936, Sep. 2008.

[11] H. J. Riblet, Discussion on "A current distribution for broadside arrays which optimizes the relationship between beamwidth and side-lobe level," *Proc. IRE*, pp.489-492, May 1947.